Unoccupied states in Cu and Zn octaethyl-porphyrin and phthalocyanine

Peter L. Cook,[1] Wanli Yang,[2] Xiaosong Liu,[1,2] Juan María García-Lastra,[3] Angel Rubio,[3] and F. J. Himpsel[1,a)]

[1]*Physics Department, University of Wisconsin Madison, 1150 University Ave., Madison, Wisconsin 53706, USA*
[2]*Advanced Light Source, Lawrence Berkeley National Laboratory, Berkeley, California 94720, USA*
[3]*Dpto. Física de Materiales, Nano-Bio Spectroscopy Group and ETSF Scientific Development Centre, Centro de Física de Materiales CSIC-UPV-MPC and DIPC, Universidad del País Vasco, Av. Tolosa 72, E-20018 San Sebastián, Spain*

(Received 8 April 2011; accepted 2 May 2011; published online 26 May 2011)

Copper and zinc phthalocyanines and porphyrins are used in organic light emitting diodes and dye-sensitized solar cells. Using near edge x-ray absorption fine structure (NEXAFS) spectroscopy at the Cu 2*p* and Zn 2*p* edges, the unoccupied valence states at the Cu and Zn atoms are probed and decomposed into 3*d* and 4*s* contributions with the help of density functional calculations. A comparison with the N 1*s* edge provides the 2*p* states of the N atoms surrounding the metal, and a comparison with inverse photoemission provides a combined density of states. © *2011 American Institute of Physics*. [doi:10.1063/1.3592937]

I. INTRODUCTION

Cu and Zn phthalocyanines (Pc) have been used as a light absorber or emitter in a variety of opto-electronic devices, such as organic light emitting diodes and dye-sensitized solar cells,[1–5] as well as photocatalytic devices.[6] They also are part of molecular donor-acceptor assemblies that serve as prototype structures for real solar cells.[5,7–10] Therefore there has been a long-standing interest in their energy level structure using both theory and various spectroscopic methods. X-ray absorption spectroscopy of the transition metal 2*p*-to-3*d* edges has been used to identify the oxidation state and other electronic properties at the site of the central metal atom, and the N 1*s*-to-2*p* edge provides information about the surrounding nitrogen cage, which generally forms the lowest unoccupied molecular orbital (LUMO). The metal 2*p* edges have been investigated systematically in Ref. 11 and the N 1*s* edge in Ref. 12. Individual results can be found in Refs. 13–23 for Cu phthalocyanine, in Refs. 19–21,24, and 25 for Zn phthalocyanine, and in Refs. 26–28 for Zn porphyrin. For the crystallographic structure, see Refs. 29–31 for Cu phthalocyanine and Ref. 32 for Zn phthalocyanine. While the 2*p* edges of transition metals, including copper, have been studied extensively, the Zn 2*p* edge has received little attention. One does not expect a transition into empty 3*d* states, since the 3*d* shell is nominally filled for divalent Zn. In Zn-Pc, for example, the 3*d* levels lie at ∼11 eV below E_F and in Zn metal at ∼10 eV below E_F.[33,34] Furthermore, the Zn 2*p* edge lies in a spectral region, where it is difficult to maintain both high resolution and high intensity, because neither gratings nor crystals work well as monochromators. Therefore we focus in this work on Zn phthalocyanine and porphyrin. The corresponding Cu compounds are investigated in parallel for comparison. In addition to the LUMO and higher-lying unoccupied energy levels, we determine the widths of the spectral features, which provides the lifetime of the unoccupied states. The orbital character is assigned with the aid of ground state calculations of the density of states projected onto the metal 3*d*, metal 4*s*, and nitrogen 2*p* states.

II. EXPERIMENTAL

Near edge x-ray absorption fine structure (NEXAFS) spectroscopy was performed with copper and zinc phthalocyanine and octaethyl-porphyrin (OEP). These chemicals were obtained as powders from Sigma-Aldrich. The powder was sublimed in ultrahigh vacuum from a tantalum Knudsen cell onto silicon wafers passivated by their native oxides. Typical sublimation temperatures were ∼460 °C for a Pc and ∼270 °C for an OEP. The temperature of the Knudsen cell was monitored with a thermocouple with an accuracy of ±10 °C. For high purity films a shutter blocked the initial more volatile impurities from being deposited.

The sample preparation was optimized at the Synchrotron Radiation Center (SRC) using the sharpness of the N 1*s* absorption edge as criterion.[11,12] The metal 2*p* and N 1*s* edges were measured at Beamline 8.0 at the Advanced Light Source (ALS) in the total electron yield mode. No radiation damage was observed after expanding the illuminated spot to ∼3 × 5 mm^2. For details on radiation-induced changes see Ref. 35.

The photon energy scale was calibrated using two points with a linear interpolation in wavelength to accurately represent the $2p_{3/2}$ and $2p_{1/2}$ peak positions. The Cu 2*p* edge was calibrated using the $2p_{3/2}$ and $2p_{1/2}$ peaks of CuO at 931.3 and 951.1 eV, respectively.[36,37] This calibration puts the Cu $2p_{3/2}$ of Cu-Pc 0.3 eV higher than in our previous work,[11] which at the Cu edge relied on other literature values.[23] The Zn 2*p* edge was calibrated using the XPS binding energies of freshly scraped zinc metal for the $2p_{3/2}$ and $2p_{1/2}$ core levels at 1021.8 eV and 1244.8 eV.[38] An alternative calibration of the Zn 2*p* edge using CuO agrees within 0.1 eV. The

a)Author to whom correspondence should be addressed. Electronic mail: fhimpsel@facstaff.wisc.edu.

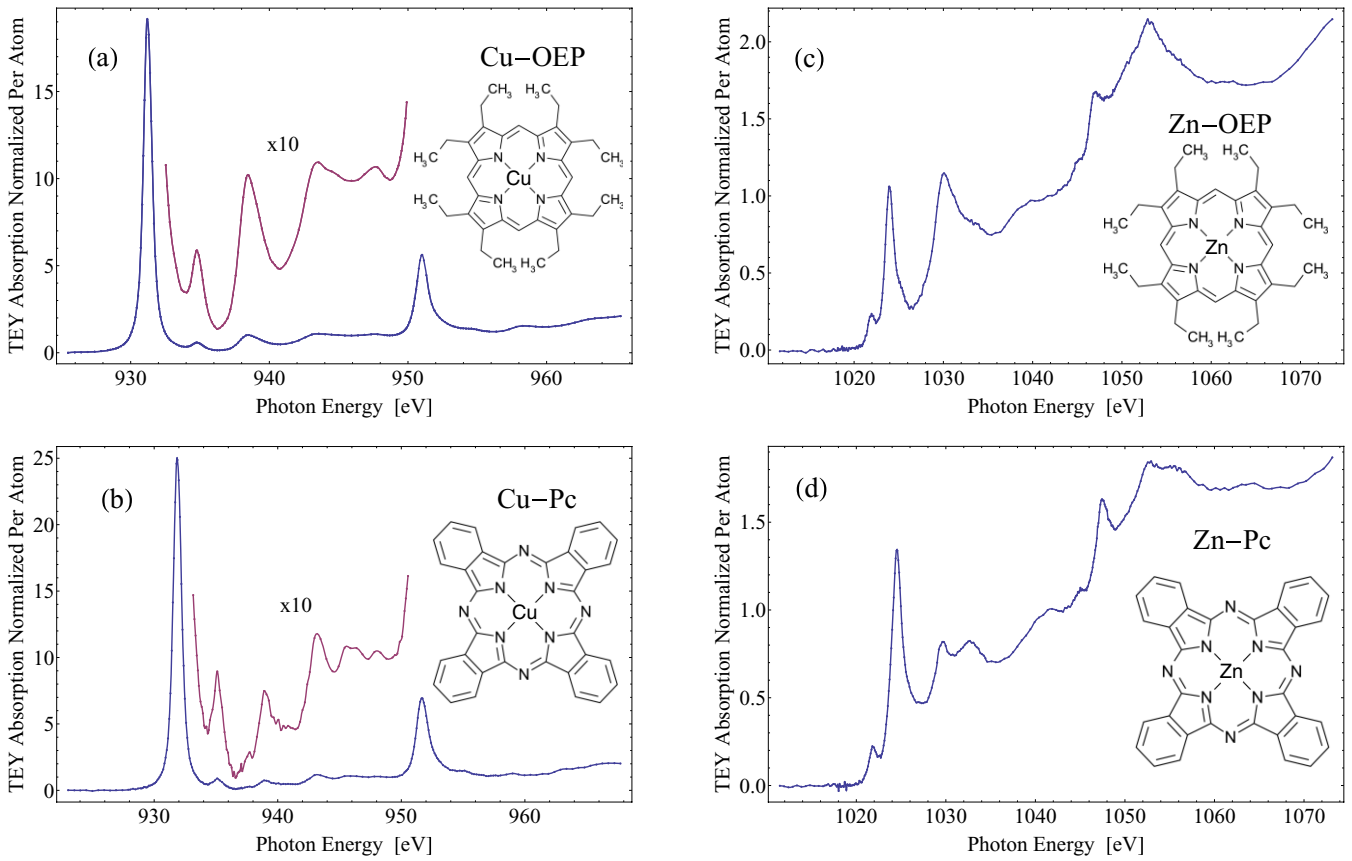

FIG. 1. The metal 2*p* edge of Cu (left) and Zn (right) octaethyl porphyrin (top) and phthalocyanine (bottom). The Cu spectra are dominated by a pair of sharp transitions from the $2p_{3/2}$ and $2p_{1/2}$ levels into the 3*d* hole of Cu^{2+} at ~931 and ~951 eV. These are absent in the Zn spectra because the 3*d* shell is filled. The remaining much weaker transitions are assigned to nitrogen 2*p* and metal 4*s* states with very little metal 3*d* character.

absolute accuracy of the photon energies is about ±0.3 eV, the relative accuracy between spectra at the same edge is about ±0.1 eV.

The sample current is first divided by the current from an Au mesh in the beamline to account for changes in the x-ray flux. A linear fit based on the pre-edge region is then subtracted from the data to remove the background caused by transitions from shallower core levels and valence states. Finally, the data are normalized approximately to the absorption per Cu or Zn atom by setting the step height from the pre-edge to the region just below the $2p_{1/2}$ peak to unity.

III. Cu AND Zn 2p NEXAFS SPECTRA

Figure 1 shows the 2*p* absorption edges of Cu and Zn octaethyl porphyrin (a and b) in comparison to those of Cu and Zn phthalocyanine (c and d). In all four spectra the spin-orbit splitting can be seen as the first half of the spectra roughly repeats itself in the second half, but with a lower intensity.

The most prominent features in the Cu 2*p* spectra are the sharp Cu 2*p*-to-3*d* transitions, whose transition matrix element is enhanced by the strong overlap between the localized 3*d* states and the 2*p* states, as well as by the higher multiplicity of the ℓ-to-(ℓ+1) transition (compared to the ℓ-to-($\ell-1$) transitions into 4*s* states). The 3*d* peak is more than an order of magnitude higher than the rest of the spectrum. Since Cu is in the +2 oxidation state in these molecules, there is a single 3*d* hole available as final state for the optical transition. Therefore, one observes only a single, sharp 2*p*-to-3*d* transition similar to that observed in CuO and other divalent Cu compounds.[37,39] At higher energies, one finds a series of weak features which eventually merge into a nearly continuous spectrum. These are assigned to a combination of metal 4*s* states and N 2*p* states from the surrounding organic ring.

The Zn 2*p* edge in Fig. 1 (c and d) lacks the strong 3*d* transition, but still contains rich spectral features analogous to the weaker transitions of the Cu-based molecules. The Zn 2*p* transitions into the LUMO and LUMO+1 at ~1022 and 1024 eV are surprisingly sharp, with a FWHM of 0.7–1.2 eV that is comparable to the FWHM of ~0.6 eV for the Cu 2*p*-to-3*d* transitions. While one expects a Cu 2*p*-to-3*d* transition for Cu^{2+} due to the single hole left in the 3*d* shell, one would not expect it for the filled 3*d* shell of Zn^{2+}. This raises the question whether hybridization gives the LUMO and LUMO+1 some Zn 3*d* character. This question will be pursued further in Sec. IV.

An interesting feature of the Zn 2*p* edges is a small peak at 1021.9 eV, which lies slightly above the binding energy of metallic zinc at 1021.8 eV.[38] The position and amplitude of this peak is nearly identical for Zn-OEP and Zn-Pc, so it is likely due to the interaction between the Zn atom and the surrounding four N atoms.

There is a systematic upwards shift in the position of the dominant 2*p* transition from Pc to OEP (i.e., the $2p_{3/2}$ peaks at

931.16, 931.88, 1023.96, and 1024.53 eV for Cu-OEP, Cu-Pc, Zn-OEP, and Zn-Pc, respectively). The corresponding energy differences are 0.6 eV (Zn), 0.7 eV (Cu), and 0.5 eV (Ni).[11,40] This shift can be explained by an additional electron transfer from the metal to the extra four nitrogens in the Pc, which increases the binding energy of the metal 2*p* core level. The charge transferred to the N atoms shifts the N 1*s* core levels in the opposite direction. This is consistent with the systematic shift of the N 1*s* edge of porphyrins containing various transition metals.[12]

IV. COMPARISON BETWEEN DIFFERENT SPECTROSCOPIES

In order to obtain experimental information about the orbital character of the unoccupied states (e.g., metal versus N), we compare the metal 2*p* edge with the N 1*s* edge in Fig. 2. In addition we use published inverse photoemission data from Refs. 41 and 42 to obtain an approximate measure of the total density of states. The energy scales have been arbitrarily aligned to the lowest observed feature. Thereby we neglect the additional energy shift due to electron-hole interaction, which mainly affects the LUMO transition. For the higher transitions, the electron-hole interactions become weaker because the kinetic energy exceeds the electron-hole interaction.

The spectra from the N 1*s* edge and from inverse photoemission are rather similar. One can draw a correspondence between nearly all peaks, as indicated by the vertical dashed lines in Fig. 2. The Cu 2*p* and Zn 2*p* spectra, however, show few common features within the first 5 eV above threshold. This can be explained by their minority character, combined with a substantial electron-hole interaction in copper. Only at energies above 5 eV, the metal and nitrogen spectra seem to approach each other (see dashed lines). This is due to the increasing delocalization of the wavefunctions at higher energies. These observations are consistent with the notion that the metal 2*p* edge projects out a single atom, while the N 1*s* edge and inverse photoemission represent the extended π system that encompasses many N and C atoms.

V. ENERGY DEPENDENT LINEWIDTH AND LIFETIME

The lifetime of electrons and holes in dye-sensitized solar cells is an important factor for their quantum efficiency.[43,44] It is possible to obtain an estimate of the electron lifetime from the lifetime broadening of the LUMO peak in NEXAFS. The energy dependent lifetime broadening also facilitates the comparison with theory, since the calculations do not include the lifetime broadening of the energy levels. Therefore we have made an attempt to extract the intrinsic lifetime broadening from the metal 2*p* edges. The width of a feature is determined by the lifetime broadening of the core hole and the electron in the unoccupied state (both Lorentzian), combined with inhomogeneous broadening, vibrational broadening, and other unresolved fine structure of an energy level (approximated by a Gaussian). The corresponding fit curves to the metal 2*p* spectra are given in Fig. 3. A step function (hyperbolic tangent) was added to account for the increasing number of weak, unresolved lines at higher energies (see Sec. VI).

Given the large number of parameters needed to fit these spectra, only the sharpest and strongest features are selected

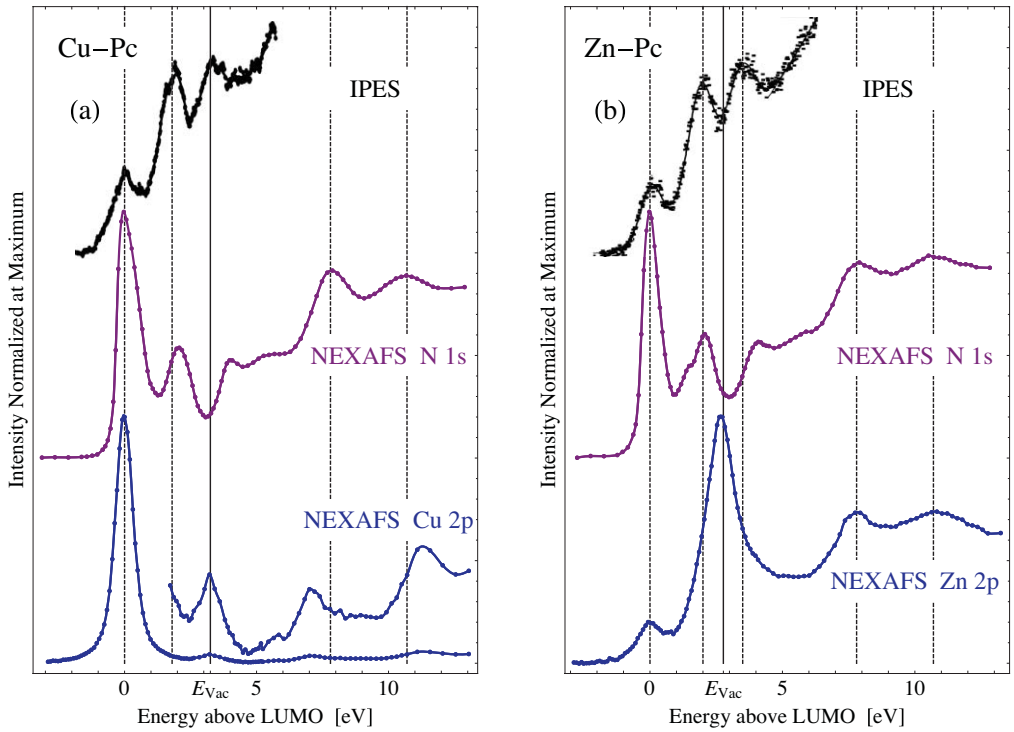

FIG. 2. Different experimental projections of the density of unoccupied states, obtained from the metal 2*p* edge, the N 1*s* edge, and inverse photoemission (reproduced from Ref. 41 for Cu-Pc and from Ref. 42 for Zn-Pc).

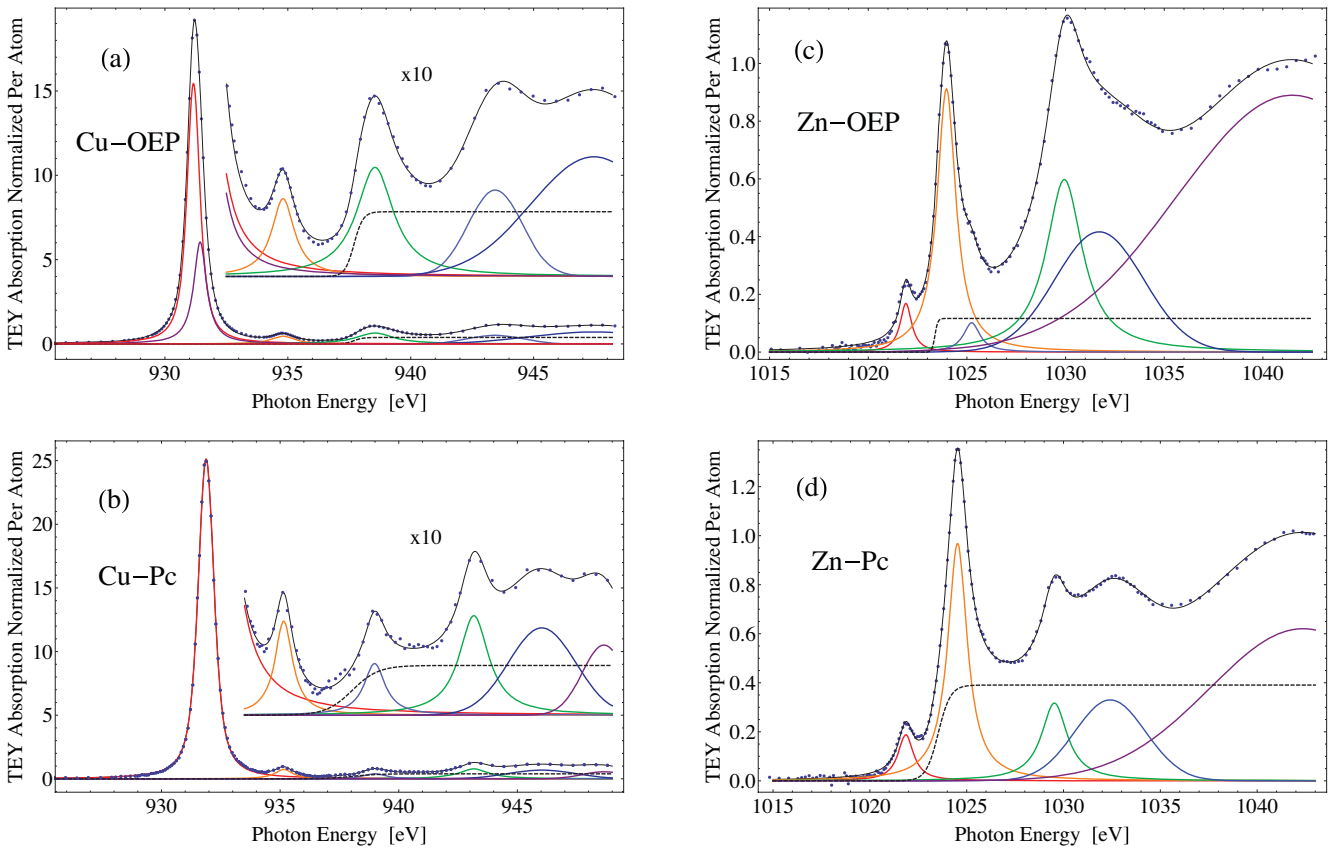

FIG. 3. Determination of the lifetime broadening Γ of the unoccupied states by fitting the sharpest $2p_{3/2}$ spectral features in Fig. 1. The line through the data is the sum of the features below. The peak widths increase linearly with energy as shown in Fig. 4.

for extracting the Lorentzian lifetime broadening. The result is plotted in Fig. 4 versus the excess energy above the LUMO transition (x axis same as in Fig. 2). An approximately linear behavior of the Lorentzian lifetime broadening is found. The intercept at the LUMO position is dominated by the inverse lifetime of the core hole, while the slope reveals the increasing lifetime broadening of the excited electron at higher energies. An approximate value of the electron lifetime broadening can be obtained by subtracting the intercept in Fig. 4. The lifetime τ is obtained from the lifetime broadening Γ via $\tau = \hbar/\Gamma$. A further observation in Fig. 4 is the larger slope of OEP compared to Pc. The magnitude of the lifetime broadening is consistent with the values obtained from the final state lifetime broadening of angle-resolved photoemission of Cu (Ref. 45) and Al (Ref. 46), and from low-energy electron diffraction (LEED) at comparable energies.

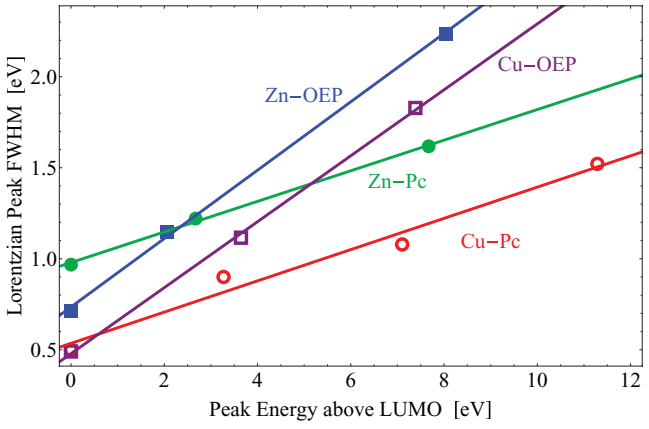

FIG. 4. The Lorentzian peak broadening (FWHM) versus the excess energy above the LUMO, obtained from the fits in Fig. 3. It increases linearly with the energy. The LUMO energy is 931.2, 931.9, 1021.9, and 1021.9 for Cu-OEP, Cu-Pc, Zn-OEP, and Zn-Pc, respectively. These results are used to realistically broaden theoretical energy levels in Fig. 5. Cu has open symbols, Zn has filled symbols, Pc has circles, and OEP has squares.

VI. ORBITAL CHARACTER FROM THE DENSITY OF STATES

In order to obtain further information about the orbital character of the unoccupied states, we use the projected density of states obtained from first principles density functional theory in the local density approximation (LDA) (Fig. 5). In contrast to the experiments discussed in Sect. IV, these calculations describe the neutral ground state, while inverse photoemission represents a negative ion state and absorption spectroscopy an excited neutral state containing an electron-hole pair. Calculations of such excited states are much more complex. They will be addressed in a future publication.[47] Although the ground state density of states shown in Fig. 5 cannot be expected to reflect the spectroscopy results, it represents important information for the chemistry of these molecules. Particularly interesting in the context of solar cells is the attachment chemistry to acceptor materials, such as

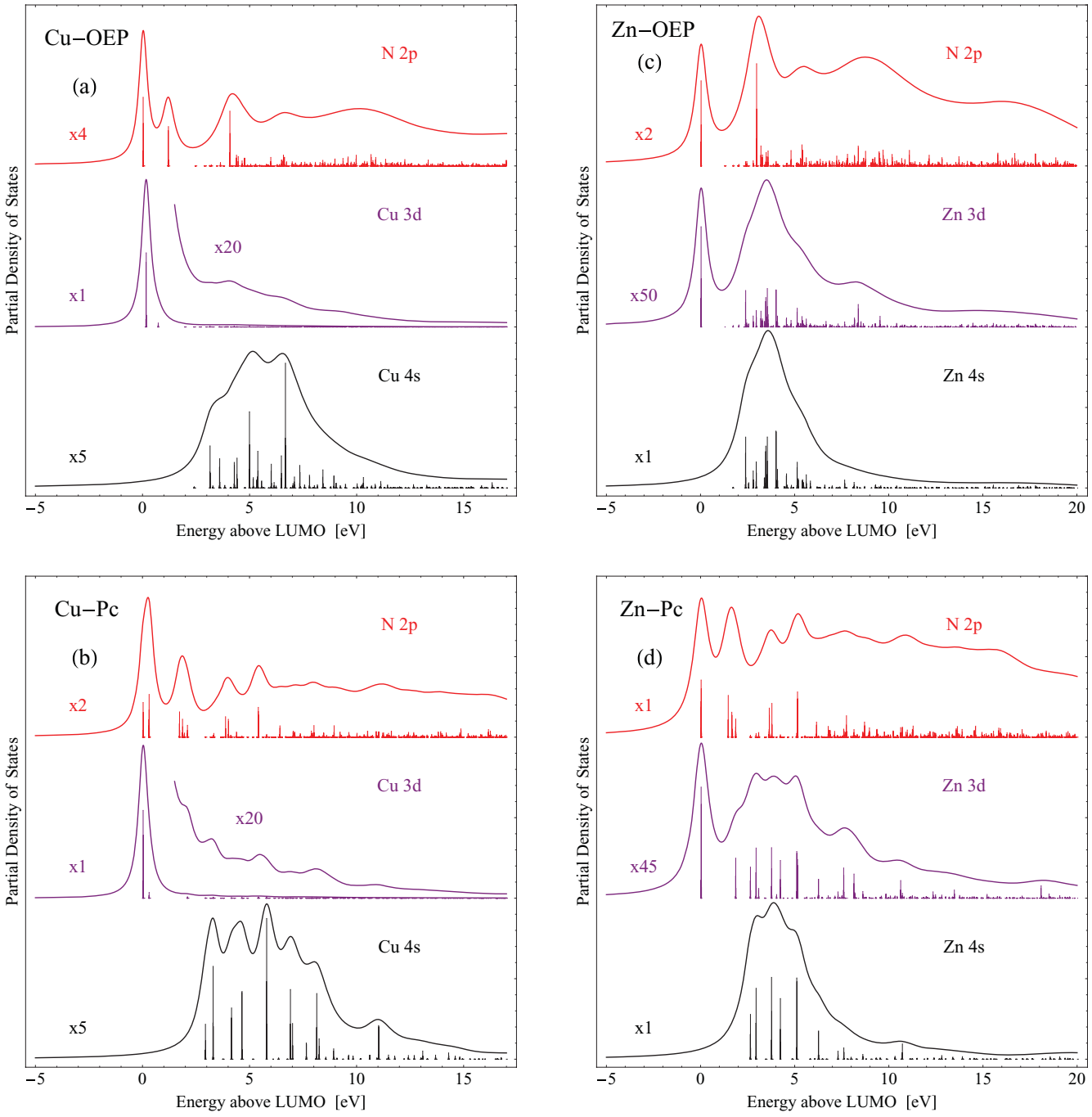

FIG. 5. Partial density of unoccupied states calculated for the ground state by LDA. For Cu-Pc and Zn-Pc, the N 2*p* contributions from the inner and outer rings of nitrogens are similar to each other and have been added.

TiO_2 and ZnO,[48,49] and the transport of excited carriers from the dye molecule.[43]

At the Cu 2*p* and Zn 2*p* edges, dipole selection rules allow transitions into 3*d* and 4*s* valence states (plus the continuum). A combination of N 2*p* valence orbitals with *d*- or *s*-like symmetry about the metal atom is allowed as well, although it may be suppressed by the low amplitude of the N 2*p* orbitals at the position of the metal atom, where the 2*p* core wave function is located. Figure 5 shows these three different projections of the unoccupied density of states (nitrogen 2*p*, metal 3*d*, and metal 4*s*).

In Cu-OEP and Cu-Pc, the LUMO has predominately Cu 3*d* character, as expected from the existence of a 3*d*-hole in Cu^{2+}. In Cu-OEP, the LUMO+1 is separated by 1.2 eV from the LUMO, while it is much closer in Cu-Pc (∼0.3 eV).

In Zn-OEP and Zn-Pc, the Zn 3*d* contribution is nearly absent because the 3*d* shell is filled. The LUMO has almost entirely N 2*p* character. It is possible to compare the LUMO in Zn-OEP with the LUMO+1 of Cu-OEP. This comparison extends even to the LUMO+1 in Zn-OEP and LUMO+2 in Cu-OEP. This similarity is supported by the strong nitrogen character and the splitting of ∼3 eV.

Apart from the LUMO in Cu-OEP and Cu-Pc, the unoccupied states of all four molecules have strong N 2*p* character. The density of states per nitrogen atom is comparable, leading to twice the density of states in the phthalocyanines than the porphyrins. The metal 4*s* states have a relatively narrow energy distribution centered at about 5 eV above threshold, while the N 2*p* states cover the whole energy range. The higher lying metal 3*d* states are insignificant.

VII. CONCLUSIONS

In summary, the unoccupied states and their lifetimes of Cu and Zn phthalocyanines and porphyrins have been investigated, with an emphasis on determining the change of their orbital character as the 3*d* shell fills up. The most dramatic difference between Cu- and Zn-containing molecules is the disappearance of the Cu 3*d* hole in Zn. Apart from this effect, the electronic structure is very similar. At both 2*p* absorption edges, a weak but highly structured density of states is found.

A comparison of the metal 2*p* with the N 1*s* edges reveals that the unoccupied states located at the metal atom and at the surrounding N atoms are very different.

The detailed projections onto the N 2*p*, the metal 3*d*, and the metal 4*s* states are obtained for the ground state from density functional calculations. In Cu-OEP and Cu-Pc the LUMO has predominantly Cu 3*d* character, while it has N 2*p* character in Zn-OEP and Zn-Pc. Unoccupied states above the LUMO are predominantly N 2*p* states with significant metal 4*s* states concentrated in a resonance ~5 eV above the LUMO.

Since Cu and Zn phthalocyanines have been used frequently in organic LEDs and solar cells, this information is relevant to electron injection and extraction in organic optoelectronics.

Future avenues to explore are time-resolved measurements of the LUMO and its lifetime via two-photon photoemission,[50,51] and custom-designed variations of porphyrins and phthalocyanines.[48,52]

ACKNOWLEDGMENTS

This work was supported by the NSF (Award Nos. CHE-1026245 and DMR-0537588 (SRC)) and by the DOE (Contract Nos. DE-FG02-01ER45917 (end station) and DE-AC03-76SF00098 (ALS)).

J.M.G.L. and A.R. acknowledge financial support from Spanish MEC (FIS2007-65702-C02-01), ACI-Promociona (ACI2009-1036), Grupos Consolidados UPV/EHU del Gobierno Vasco (IT-319-07), the European Union through the FP7 e-I3 ETSF (Contract No. 211956), and THEMA (Contract No. 228539) projects. They also acknowledge support by the Barcelona Supercomputing Center, Red Española de Supercomputación, ARINA and NABIIT.

[1] A. Hagfeldt, G. Boschloo, L. Sun, L. Kloo, and H. Pettersson, Chem. Rev. **110**, 6595 (2010).
[2] J.-H. Yum, S. R. Jang, R. Humphry-Baker, M. Grätzel, J.-J. Cid, T. Torres, and M. K. Nazeeruddin, Langmuir **24**, 5636 (2008).
[3] W. M. Campbell, K. W. Jolley, P. Wagner, K. Wagner, P. J. Walsh, K. C. Gordon, L. Schmidt-Mende, M. K. Nazeeruddin, Q. Wang, M. Grätzel, and D. L. Officer, J. Phys. Chem. C **111**, 11760 (2007).
[4] T. Bessho, S. Zakeeruddin, C.-Y. Yeh, E.-G. Diau, and M. Grätzel, Angew. Chem., Int. Ed. **49**, 6646 (2010).
[5] C. Hein, E. Mankel, T. Mayer, and W. Jaegermann, Sol. Energy Mater. Sol. Cells **94**, 662 (2010).
[6] D. Schaming, R. Farha, H. Xu, M. Goldmann, and L. Ruhlmann, Langmuir **27**, 132 (2011).
[7] D. G. de Oteyza, I. Silanes, M. Ruiz-Oses, E. Barrena, B. P. Doyle, A. Arnau, H. Dosch, Y. Wakayama, and J. E. Ortega, Adv. Funct. Mater. **19**, 259 (2009).
[8] D. G. de Oteyza, J. M. García-Lastra, M. Corso, B. P. Doyle, L. Floreano, A. Morgante, Y. Wakayama, A. Rubio, and J. E. Ortega, Adv. Funct. Mater. **19**, 3567 (2009).
[9] S. W. Cho, L. F. J. Piper, A. DeMasi, A. R. H. Preston, K. E. Smith, K. V. Chauhan, P. Sullivan, R. A. Hatton, and T. S. Jones, J. Phys. Chem. C **114**, 1928 (2010).
[10] S. W. Cho, L. F. J. Piper, A. DeMasi, A. R. H. Preston, K. E. Smith, K. V. Chauhan, R. A. Hatton, and T. S. Jones, J. Phys. Chem. C **114**, 18252 (2010).
[11] P. L. Cook, X. Liu, W. Yang, and F. J. Himpsel, J. Chem. Phys. **131**, 194701 (2009).
[12] J. M. García-Lastra, P. L. Cook, F. J. Himpsel, and A. Rubio, J. Chem. Phys. **133**, 151103 (2010).
[13] A. Ruocco, F. Evangelista, R. Gotter, A. Attili, and G. Stefani, J. Phys. Chem. C **112**, 2016 (2007).
[14] M. Gorgoi and D. R.T. Zahn, Org. Electron. **6**, 168 (2005).
[15] R. Resel, M. Ottmar, M. Hanack, J. Keckes, and G. Leising, J. Mater. Res. **15**, 934 (2000).
[16] L. F. J. Piper, S. W. Cho, Y. Zhang, A. DeMasi, K. E. Smith, A. Y. Matsuura, and C. McGuinness, Phys. Rev. B **81**, 045201 (2010).
[17] N. Marom, O. Hod, G. E. Scuseria, and L. Kronik, J. Chem. Phys. **128**, 164107 (2008).
[18] J. E. Downes, C. McGuinness, P.-A. Glans, T. Learmonth, D. Fu, P. Sheridan, and K. E. Smith, Chem. Phys. Lett. **390**, 203 (2004).
[19] L. Zhu, H. Tang, Y. Harima, Y. Kunugi, K. Yamashita, J. Ohshita, and A. Kunai, Thin Solid Films **396**, 214 (2001).
[20] H. Yoshida, K. Tsutsumi, and N. Sato, J. Electron Spectrosc. Relat. Phenom. **121**, 83 (2001).
[21] M.-S. Liao and S. Scheiner, J. Chem. Phys. **114**, 9780 (2001).
[22] S. Carniato, Y. Luo, and H. Ågren, Phys. Rev. B **63**, 085105 (2001).
[23] G. Dufour, C. Poncey, F. Rochet, H. Roulet, M. Sacchi, M. De Santis, and M. De Crescenzi, Surf. Sci. **319**, 251 (1994).
[24] U. Weiler, T. Mayer, W. Jaegermann, C. Kelting, D. Schlettwein, S. Makarov, and D. Wöhrle, J. Phys. Chem. B **108**, 19398 (2004).
[25] D. Schlettwein, K. Hesse, N. E. Gruhn, P. A. Lee, K. W. Nebesny, and N. R. Armstrong, J. Phys. Chem. B **105**, 4791 (2001).
[26] N. Schmidt, R. Fink, and W. Hieringer, J. Chem. Phys. **133**, 054703 (2010).
[27] S. Narioka, H. Ishii, Y. Ouchi, T. Yokoyama, T. Ohta, and K. Seki, J. Phys. Chem. **99**, 1332 (1995).
[28] G. Polzonetti, V. Carravetta, G. Iucci, A. Ferri, G. Paolucci, A. Goldoni, P. Parent, C. Laffon, and M. V. Russo, Chem. Phys. **296**, 87 (2004).
[29] M. A. Shaibat, L. B. Casabianca, D. Y. Siberio-Prez, A. J. Matzger, and Y. Ishii, J. Phys. Chem. B **114**, 4400 (2010).
[30] A. Hoshino, Y. Takenaka, and H. Miyaji, Acta Cryst. **59**, 393 (2003).
[31] S. Tokito, J. Sakata, and Y. Taga, Thin Solid Films **256**, 182 (1995).
[32] W. Dou, Y. Tang, C. S. Lee, S. N. Bao, and S. T. Lee, J. Chem. Phys. **133**, 144704 (2010).
[33] M. Iwan, E. E. Koch, T.-C. Chiang, and F. J. Himpsel, Phys. Lett. A **76**, 177 (1980).
[34] F. J. Himpsel, D. E. Eastman, E. E. Koch, and A. R. Williams, Phys. Rev. B **22**, 4604 (1980).
[35] P. L. Cook, P. S. Johnson, X. Liu, A.-L. Chin, and F. J. Himpsel, J Chem. Phys. **131**, 214702 (2009).
[36] K. Shimizu, H. Maeshima, H. Yoshida, A. Satsuma, and T. Hattori, Phys. Chem. Chem. Phys. **3**, 862 (2001).
[37] M. Grioni, J. B. Goedkoop, R. Schoorl, F. M. F. de Groot, and J. C. Fuggle, Phys. Rev. B **39**, 1541 (1989).
[38] A. Lebugle, U. Axelsson, R. Nyholm, and N. Mårtensson, Phys. Scr. **23**, 825 (1981).
[39] M. Iwan, E. E. Koch, T.-C. Chiang, D. E. Eastman, and F. J. Himpsel, Solid State Commun. **34**, 57 (1980).

[40]S. A. Krasnikov, A. B. Preobrajenski, N. N. Sergeeva, M. M. Brzhezinskaya, M. A. Nesterov, A. A. Cafolla, M. O. Senge, and A. S. Vinogradov, Chem. Phys. **332**, 318 (2007).
[41]I. G. Hill, A. Kahn, Z. G. Soos, and R. A. Pascal,Jr., Chem. Phys. Lett. **327**, 181 (2000).
[42]W. Gao and A. Kahn, Org. Electron. **3**, 53 (2002).
[43]S. Meng and E. Kaxiras, Nano Lett. **10**, 1238 (2010).
[44]J. Fortage, E. Göransson, E. Blart, H.-C. Becker, L. Hammarström, and F. Odobel, Chem. Commun. **44**, 4629 (2007).
[45]D. E. Eastman, J. A. Knapp, and F. J. Himpsel, Phys. Rev. Lett **41**, 825 (1978).
[46]H. J. Levinson, F. Greuter, and E. W. Plummer, Phys. Rev. B **27**, 727 (1983).
[47]J. M. García-Lastra, P. L. Cook, W. Yang, X. Liu, F. J. Himpsel, and A. Rubio, "Excited state vs. ground state calculations of the unoccupied electronic states of Cu and Zn porphyrins and phthalocyanines" (unpublished).
[48]R. González-Moreno, P. L. Cook, I. Zegkinoglou, X. Liu, P. S. Johnson, W. Yang, R. Ruther, R. Hamers, R. Tena-Zaera, F. J. Himpsel, J. E. Ortega, and C. Rogero, "Attachment of protoporphyrin dyes to nanostructured ZnO surfaces: Characterization by NEXAFS" (unpublished).
[49]S.-C. Li, J.-G. Wang, P. Jacobson, X.-Q. Gong, A. Selloni, and U. Diebold, J. Am. Chem. Soc. **131**, 980 (2009).
[50]D. Ino, K. Watanabe, N. Tagaki, and Y. Matsumoto, J. Phys. Chem. B **109**, 18018 (2005).
[51] D. G. Dutton, W. Jin, J. E. Reutt-Robey, and S. W. Robey, Phys. Rev. B **82**, 073407 (2010).
[52] A. Rienzo, L. C. Mayor, G. Magnano, C. J. Satterley, E. Ataman, J. Schnadt, K. Schulte, and J. N. O'Shea, J. Chem. Phys. **132**, 084703 (2010).